electronic reprint

Journal of
Applied Crystallography
ISSN 0021-8898

A method of precise misorientation determination

A. Morawiec

Journal of
Applied Crystallography
ISSN 0021-8898

Received 16 May 2003
Accepted 21 July 2003

A method of precise misorientation determination

A. Morawiec

Instytut Metalurgii i Inżynierii Materiałowej PAN, Kraków, Poland. Correspondence e-mail: nmmorawi@cyf-kr.edu.pl

A method that improves the accuracy of misorientations determined from Kikuchi patterns is described. It is based on the fact that some parameters of a misorientation calculated from two orientations are more accurate than other parameters. A procedure which eliminates inaccurate elements is devised. It requires at least two foil inclinations. The quality of the approach relies on the possibility to set large sample-to-detector distances and the availability of good spatial resolution of transmission electron microscopy. Achievable accuracy is one order of magnitude better than the accuracy of the standard procedure.

1. Introduction

Analysis of orientations plays an important role in the investigation of polycrystalline materials. Frequently, not orientations per se but relative orientations (misorientations) between crystal structures at different points of the sample are of interest. Misorientations are essential for research on grain boundaries, interphase orientation relationships and for characterization of microstructures *via* lattice curvature (*e.g.* Sun *et al.*, 2000). In many cases, especially when low-angle misorientations are considered, there are high expectations concerning accuracy of the data. Actually, what matters is the combination of accuracy and spatial resolution. Since traditional X-ray-based techniques have relatively low resolution, misorientations are usually determined using electron microscopy. Attempts have been made to investigate problems requiring high misorientation accuracy using scanning electron microscopy (SEM) with electron backscattering diffraction (EBSD) systems (Wilkinson, 2001). However, the capabilities of that approach are limited by the small sample-to-detector distance. Therefore, commercial SEM/EBSD systems with a level of random errors at about 0.5–1.0° (Krieger Lassen, 1995) are too crude to investigate subtle orientation differences. Considerably higher precision in misorientation determination is achievable using transmission electron microscopy (TEM). In the case of Kikuchi or convergent-beam diffraction patterns, the maximal error is about 0.1–0.2° (Gemperle & Gemperlová, 1995).

It is important to note here that the accuracy of the microscopic measurements of absolute orientations depends on a number of external factors (precision in cutting out the sample, quality of the sample holder, alignment of the sample in the holder). They are collectively referred to as 'sample positioning factors'. For the accuracy of a misorientation calculated from two orientations, the issue of sample positioning is immaterial if orientations are obtained under exactly the same conditions. In that case, the accuracy is limited by random errors caused by imperfect resolution of diffraction patterns.

There is a relatively extensive literature on misorientation determination using TEM (see *e.g.* Chen & King, 1987, and references therein). The procedure proposed here is related to two previously described methods that require more than just one foil inclination. The first one (Bonnet & Durand, 1975) uses patterns from the interface area, *i.e.* two Kikuchi line systems originating from two neighbouring crystallites must be visible in one pattern. Positions of zone axes of the two systems obtained at two foil inclinations are then used for calculating the misorientation between the crystallites. In the second method (Goringe *et al.*, 1979), for a number of different foil inclinations, vectors along beam directions are determined in each of the two crystallites of interest; the misorientation is represented by the best orthogonal matrix relating the two sets of vectors. Generally, the older papers do not take into account computerized methods of analysis and indexing of diffraction patterns. Nowadays, a high-quality pattern can be indexed by a computer-mouse click (Zaefferer, 2000; Morawiec *et al.*, 2002) and the output contains orientation parameters which are then used for calculating misorientations.

Such a misorientation can be seen as a composition of two components: a rotation about the axis parallel to the electron beam and a rotation about an axis perpendicular to the beam. Roughly, the accuracy of a rotation about an axis perpendicular to the beam is proportional to the effective camera length L. Moreover, the accuracy also depends on the resolution of the registered pattern δ. The maximum precision is of the order of δ/L (radians). Thus, the larger the length L is, the smaller is the error level. However, the camera length has no influence on the precision of rotations about the beam direction. It is determined by δ/Δ (radians), where Δ is the dimension of the recorded pattern. With a 1 square inch, 1024×1024 pixel resolution camera and typical thickness of Kikuchi lines of, say, 4 pixels, the ratio δ/Δ corresponds to the angular accuracy of $\sim$0.2°, whereas, for the large effective camera length of 150 cm, the ratio δ/L corresponds to $\sim$0.004°. These numbers show that in realistic conditions the precision

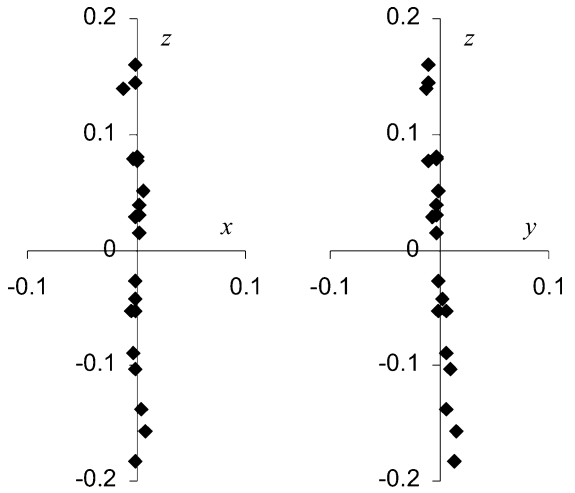

Figure 1
Deviations from the average orientation for 20 orientations determined conventionally from one diffraction pattern with L = 604 mm. The directions x and y, and the beam direction z are mutually perpendicular. Here and in Figs. 2–4, all values are given in degrees.

in misorientation determination is limited by the accuracy of the rotation about the axis parallel to the electron beam.

The above issue is illustrated in Fig. 1. The same diffraction pattern was used 20 times for orientation determination. The distribution of the 20 orientations with respect to the average orientation is shown. The points represent components of the rotation vector (*i.e.* the unit vector in the direction of the rotation axis scaled by the rotation angle). The scatter of the points represents the level of random errors. Clearly, rotations about the z direction, which was chosen to be parallel to the beam, are more affected by the errors than the rotations about other axes.

2. The method

It is possible to reduce the large random errors in rotations about the beam direction and, consequently, achieve a better overall accuracy by using a relatively simple method. Briefly, the method requires at least two orientation measurements at each point. The orientations must be obtained for different foil inclinations. Because of the tilts, the large error associated with the rotation about the beam direction influences different 'components' of the orientation. The unaffected (*i.e.* accurate) components are used for determining the misorientation. The tilt, which is associated with the sample positioning, is eliminated from the misorientation calculation.

Explicitly, the following steps need to be taken to obtain a misorientation between two (centrosymmetric) crystallites A and B: (i) for a given foil inclination, determine the orientation (special orthogonal) matrices $O_{\rm A}^1$ and $O_{\rm B}^1$ for A and B, respectively; (ii) change the sample tilt; (iii) for the new sample position, determine the orientation matrices $O_{\rm A}^2$ and $O_{\rm B}^2$ for the first crystallite and the second crystallite, respectively.

Based on the four orientations, the procedure allows high-accuracy misorientation parameters to be calculated. For even better precision, one may use more sample positions. In general, if the upper index enumerates the tilts, one has $O_{\rm A}^i$ and $O_{\rm B}^i$ for the ith tilt, with $i = 1, 2, \ldots, N$. In all cases, the setting of the camera length should be as large as possible.

Let us concentrate on the case with a given tilt i. For the first of two measurements, we can write

$$T_{\rm A} P E_{\rm A} = O_{\rm A}^i, \tag{1}$$

where $E_{\rm A}$ and $T_{\rm A}$ are the errors associated with the rotation about the beam direction and the true orientation, respectively. P represents the unknown rotation corresponding to the sample positioning (including tilt). Analogously, for the second measurement, one can write $T_{\rm B} P E_{\rm B} = O_{\rm B}^i$. Hence, the true misorientation represented by the matrix $M = T_{\rm A} T_{\rm B}^T$ is given by

$$M = O_{\rm A}^i (E^i)^T (O_{\rm B}^i)^T, \tag{2}$$

where $E^i = E_{\rm B}^T E_{\rm A}$ is the combined error rotation about the beam direction. The accuracy of the misorientation obtained directly from $O_{\rm A}^i (O_{\rm B}^i)^T$ is low because of the actual presence of the unknown factor E^i. Let $\|X - Y\|$ be a 'distance' in the rotation space. The true misorientation M can be approximated by

$$\arg_X \min_{X, E^i} \sum_{i=1}^{N} \|X - O_{\rm A}^i (E^i)^T (O_{\rm B}^i)^T\|^2, \tag{3}$$

subject to the conditions that X and E^i are special orthogonal, plus a condition specific to the experiment; in our case, the specific condition is that E^i represent rotations about the beam direction. With the norm $\|\cdot\|$ specified,[1] the problem (3) can be solved numerically.

There is an additional aspect which must be taken into account. Due to crystal symmetry, physically identical orientations or misorientations can be described by different orientation parameters. In other words, a given (mis)orientation can be determined by different but symmetrically equivalent parameters. The described method of misorientation determination will work only if the orientation parameters are chosen in a consistent way. The procedure is straightforward. Based on the tilt 1, the true misorientation is close to $M^1 := O_{\rm A}^1 (O_{\rm B}^1)^T$. If $O_{\rm A}^i$ represents the first orientation measured for the tilt $i \neq 1$, then the second one $O_{\rm B}^i$ cannot be randomly selected; from the set of symmetrically equivalent matrices, the one closest to $(M^1)^T O_{\rm A}^i$ must be taken.

3. Quaternion-based procedure

The idea of the method was presented above using orthogonal matrices because that formalism is well known. However, the calculations become more simple if the rotations are represented by unit quaternions and the distance inherited from the quaternion vector space is used. By the distance between quaternions x and y, we mean $\|x - y\|$, where $\|x\| = \left(\sum_{\kappa=0}^{3} x_\kappa x_\kappa\right)^{1/2}$ and x_κ, $(\kappa = 0, 1, 2, 3)$ is the κth component of x. Further on, xy will denote the quaternion product of x and y

[1] It can be the Frobenius norm in the linear space of matrices.

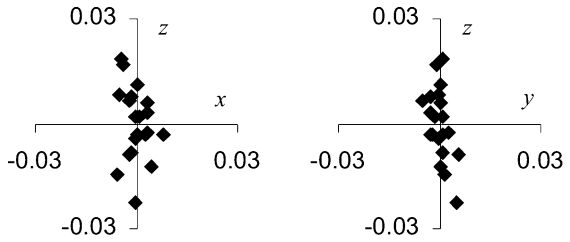

Figure 2
Misorientations with respect to the average orientation determined by the proposed accurate procedure. The parameters of the diffraction patterns used here were the same as in the case of Fig. 1.

and the quaternion conjugate to x will be denoted by x^*. One has to remember that the correspondence between unit quaternions and rotations is two-to-one; of two equivalent unit quaternions, the one closer to the identity quaternion will be used.[2] [For more on quaternions, see *e.g.* the work of Altmann (1986); a very brief account was also given by Morawiec & Pospiech (1989).]

Let the quaternions $q^i_{\rm A}$, $q^i_{\rm B}$ and e^i correspond to $O^i_{\rm A}$, $O^i_{\rm B}$ and E^i, respectively. In analogy to equation (3), the true misorientation is approximated by the quaternion

$$\arg_x \min_{q,e^i} \sum_{i=1}^{N} \| x - q^i_{\rm A} e^{i*} {q^i_{\rm B}}^* \|^2 \qquad (4)$$

under the conditions that q and e^i are unit quaternions and that e^i correspond to rotations about the beam direction. Direct calculation shows that $\|x - q^i_{\rm A} e^{i*} {q^i_{\rm B}}^*\|^2 = 2\big[1 - \sum_\kappa x_\kappa (q^i_{\rm B} e^i {q^i_{\rm A}}^*)_\kappa\big]$. The κth component $(q^i_{\rm B} e^i {q^i_{\rm A}}^*)_\kappa$ of the quaternion $q^i_{\rm B} e^i {q^i_{\rm A}}^*$ is linear with respect to the components of e^i. Thus, the expression

$$(q^i_{\rm B} e^i {q^i_{\rm A}}^*)_\kappa = \sum_\mu Q^i_{\kappa\mu} e^i_\mu \qquad (5)$$

defines N matrices Q^i. The explicit formula for Q^i is given in Appendix *A*. Now, with Λ and λ^i denoting Lagrange multipliers, the function (of x and e^i)

$$\sum_i 2\Big(1 - \sum_{\kappa,\mu} x_\kappa Q^i_{\kappa\mu} e^i_\mu\Big) + \Lambda\Big(\sum_\kappa x_\kappa x_\kappa - 1\Big) + \sum_i \lambda^i \Big(\sum_\mu e^i_\mu e^i_\mu - 1\Big) \qquad (6)$$

is stationary if

$$\sum_\kappa Q^i_{\kappa\mu} x_\kappa = \lambda^i e^i_\mu \quad \text{and} \quad \sum_{i,\mu} Q^i_{\kappa\mu} e^i_\mu = \Lambda x_\kappa. \qquad (7)$$

Substitution of x_κ in the first of these equations by the second one leads to

$$\Lambda \sum_{j,\nu} R^{ij}_{\mu\nu} e^j_\nu = \lambda^i e^i_\mu, \qquad (8)$$

where $R^{ij}_{\mu\nu} = \sum_\kappa Q^i_{\kappa\mu} Q^j_{\kappa\nu}$. Brief calculation shows that $R^{ij}_{\mu\nu} = R^{ji}_{\nu\mu}$ and $R^{ii}_{\mu\nu} = \delta_{\mu\nu}$.

With e^i representing rotations about the beam (or z) direction, only the entries with $\mu = 0, 3$ are non-zero. After omitting rows and columns consisting of zeros, R^{ij} become 2×2 matrices and our main equation (8) can be written as

$$\Lambda \begin{bmatrix} I_2 & R^{12} & R^{13} & \dots & R^{1N} \\ R^{21} & I_2 & R^{23} & \dots & R^{2N} \\ R^{31} & R^{32} & I_2 & \dots & R^{3N} \\ \vdots & \vdots & \vdots & \ddots & \vdots \\ R^{N1} & R^{N2} & R^{N3} & \dots & I_2 \end{bmatrix} \begin{bmatrix} e^1 \\ e^2 \\ e^3 \\ \vdots \\ e^N \end{bmatrix} = \begin{bmatrix} \lambda^1 e^1 \\ \lambda^2 e^2 \\ \lambda^3 e^3 \\ \vdots \\ \lambda^N e^N \end{bmatrix}, \qquad (9)$$

where I_2 is the 2×2 identity matrix and the e^i vectors have two components.

In particular, for the most interesting case of two foil inclinations ($N = 2$), the problem is reduced to two two-dimensional eigenvalue problems

$$\Lambda^2 (R^{12} R^{21}) e^1 = \lambda^1 \lambda^2 e^1, \qquad \Lambda^2 (R^{21} R^{12}) e^2 = \lambda^1 \lambda^2 e^2. \qquad (10)$$

Since the matrices $R^{12}R^{21}$ and $R^{21}R^{12}$ are symmetric, there are real solutions to the problems. Because e^i correspond to small angle rotations, the problems are solved by the eigenvectors close to $(1, 0)^T$. With known e^i, the quaternion x minimizing (6) and representing the sought misorientation is calculated from the second of equations (7) and $\|x\| = 1$.

The results of application of the proposed procedure are illustrated in Fig. 2. The orientation data were collected from diffraction patterns recorded with tilts of -20 and 20°. In analogy to Fig. 1, misorientations with respect to the average orientation are given in the form of the rotation vector. The scatter of the points and the level of random errors along the beam direction are one order of magnitude smaller than those shown in Fig. 1.

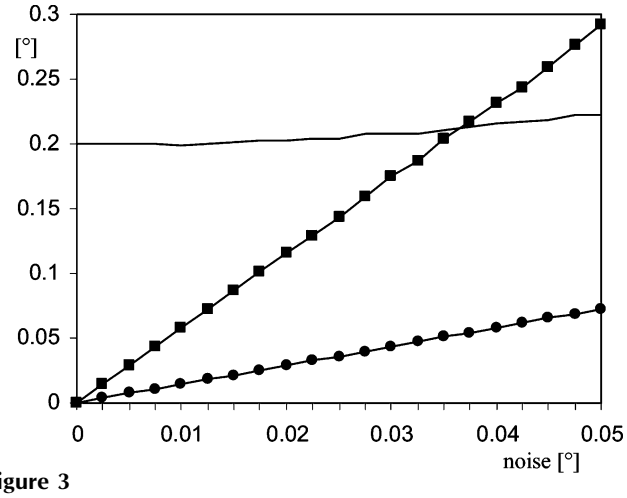

Figure 3
Maximal (squares) and average (circles) differences between the calculated and the true misorientations *versus* 'noise'. The line without markers represents the numerically estimated maximal error of misorientations determined in the conventional way.

4. Sensitivity assessment

The sensitivity of the method to experimental errors and its dependence on the tilt angle were estimated numerically. All tests were performed for cubic (O_h) crystal symmetry. Since there are a number of parameters involved, it is difficult to

[2] The cases with the two equivalent unit quaternions at the same distance to the identity are of no practical importance and will not be discussed here.

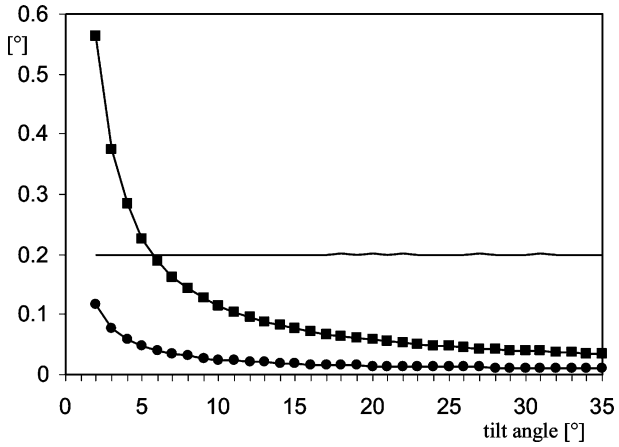

Figure 4
Maximal (squares) and average (circles) errors *versus* tilt angle. The line without markers represents the maximal error for misorientations determined in the conventional way.

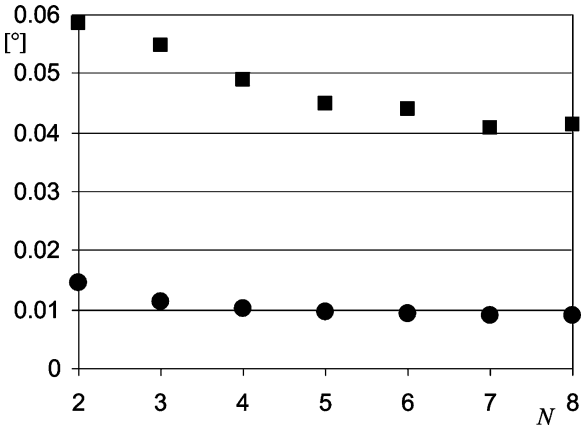

Figure 5
Maximal (squares) and average (discs) errors *versus* the number of foil inclinations. Values on the ordinate are given in degrees.

estimate the gain in accuracy globally. Sections through the parameter space give an idea of the overall behavior of the method. Fig. 3 shows the variations in the maximal and average deviations between the calculated misorientations and the true ones with inaccuracies in the rotations about axes perpendicular to the beam ('noise'). In practice, the inaccuracies are of the order of δ/L. To obtain the figure, realistic conditions were simulated by adding relatively large errors for the rotation about the beam direction and small-angle rotations for other axes. More precisely, in one step the following procedure was applied. First, two random orientations were generated, and two tilts of 20 and -20° were applied to each of them, creating a total of four orientations. Then, the orientations were modified by random errors; they were composed of four random rotations about axes perpendicular to the beam with angles not exceeding a value on the abscissa. Then, rotations about the beam direction with a random rotation angle not exceeding 0.1° were applied. These artificially biased data were the basis for calculating misorientations *via* equation (10). In Fig. 3, the ordinate represents the deviations between the 'exact' misorientations obtained from the error-free initial orientations and the misorientations calculated from (10). For each curve in Fig. 3, as well as those in Figs. 4 and 5, 10^7 steps were used. In the range we are interested in, the maximal and average errors are simply proportional to the noise.

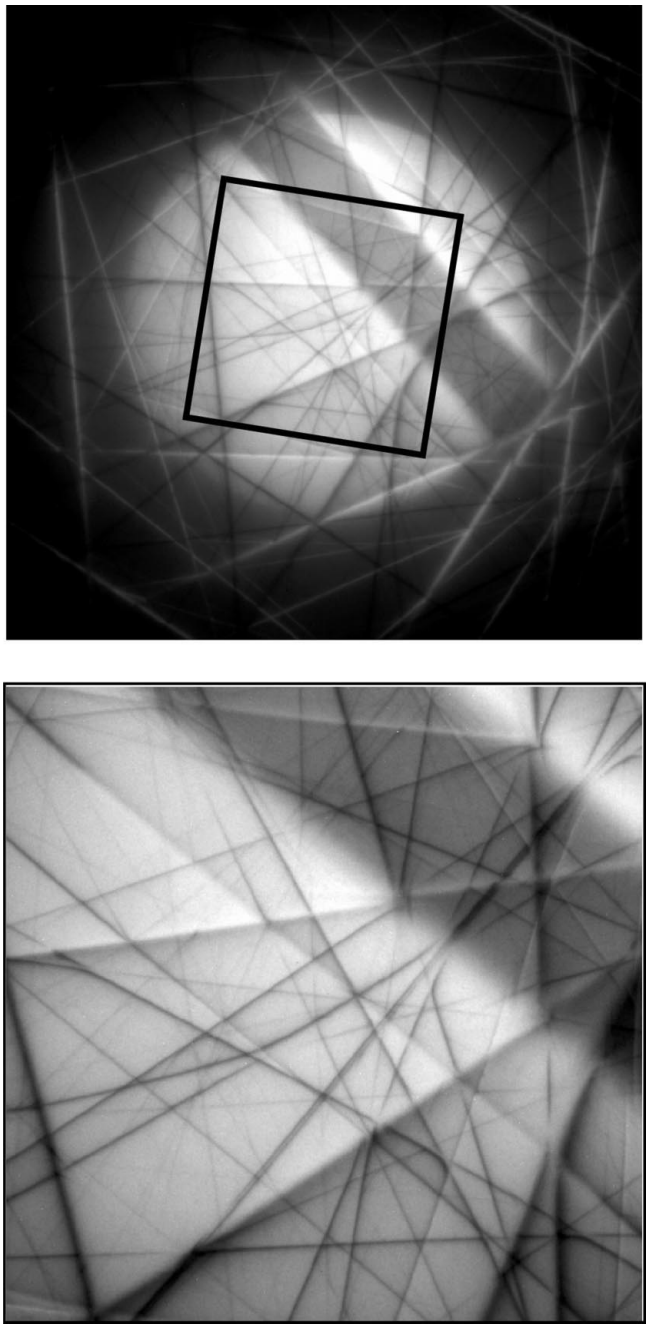

Figure 6
TEM diffraction patterns obtained with a convergent electron beam. This is one of the sets used in the tests of Figs. 1 and 2. The effective camera lengths are 225 mm and 604 mm. The first pattern is used only for indexing. Orientation parameters are determined from the second pattern.

It is interesting to take a look at the dependence of the difference between the exact and calculated misorientations on the magnitude of the tilt. Obviously the described proce-

dure breaks down if the tilt is small. The maximal and average differences (between the recalculated and the true misorientations) *versus* the tilt angle are shown in Fig. 4. The tilt angles were plus and minus the value on the abscissa, *i.e.* the total difference in the foil inclination is two times that value. As before, random errors were added to generated random orientations. The angles of error rotations about axes perpendicular to the beam did not exceed 0.01°. The rotations about the beam direction were not larger than 0.1°. The figure shows that a gain in accuracy is possible only for tilts larger than a certain cut-off value.

Figs. 3 and 4 were obtained for $N = 2$. Slightly better accuracy can be achieved by using a larger number of foil inclinations. This is illustrated in Fig. 5, showing the average and maximal error *versus* N. The axes of the tilt rotations were symmetrically distributed in the plane perpendicular to the beam direction. In all cases, the magnitude of the inclination was 20°. The levels of random errors added to the generated orientations were the same as in the case of Fig. 4. To obtain the presented data, equation (9) was solved with respect to e^i using an iteration method. Initially, the vectors e^i were set at $(1, 0)^T$. At each step, the current set of e^i vectors was put into the left side of (9) and then the calculation of the right side, plus normalization, provided a new set of vectors. The iteration was stopped when the magnitude of the deviation between the current and the new e^i vectors became smaller than 10^{-12} for all i.

5. Final remarks

The described approach requires large camera lengths. This means that the solid angle covered by the pattern detector becomes small. For a very high precision in misorientation determination, the angle is too small for pattern indexing. The problem can be easily overcome by collecting a couple of patterns for gradually increasing camera lengths (Fig. 6). The patterns corresponding to the small values of the camera length are used for reliable indexing. Once the indexing and a rough orientation are known, the patterns obtained with the large camera length are used for fine tuning the orientation parameters.

The proposed method is based on the assumption that the diffraction patterns are collected from two points with unique orientations. In reality, because of finite thickness of the foil and finite probe size, the patterns originate from certain volumes in which the orientation field may vary. With the new high-precision procedure, the volumes are additionally increased by the necessity of inclining the foil. In some cases, this loss in spatial resolution may outweigh the gain in accuracy. Therefore, one should not expect the new method to be universal. It is applicable only to materials in which the volumes affecting the patterns are characterized by unique orientations.

Results of the proposed procedure can be corrupted by shifts of the pattern centre (the geometrical point of the intersection of the detector plane with the line perpendicular to the plane through the sample point from which the diffraction originates). The centre is allowed to be at different locations for the points A and B, but it must be fixed for all patterns corresponding to each of these points. Otherwise, corrections will be needed.

Quaternions constitute a convenient parameterization for the proposed method. Application of other parameterizations of the orientation space may be considered but one has to be careful about singularities. For example, it does not make sense to analyse rotation axes for small-angle rotations because the axis/angle parameterization is singular at the point of zero rotation angle (Prior, 1999; Wilkinson, 2001).

The described method takes advantage of the high accuracy of some orientation components. The principle used here is applicable in other experimental situations, in which the presence of inaccurate components negatively influences the overall precision of the misorientation determination.

APPENDIX *A*
Explicit formula for Q^i

The entries of the matrix Q^i are calculated by expanding the left side of the relation $(q^i_{\rm B} e^i q^{i\,*}_{\rm A})_\kappa = \sum_\mu Q^i_{\kappa\mu} e^i_\mu$. Simple calculation shows that the coefficients of e^i_μ are

$$
\begin{aligned}
Q^i_{00} &= \sum_\kappa (q^i_{\rm A})_\kappa (q^i_{\rm B})_\kappa,\\
Q^i_{0m} &= (q^i_{\rm A})_m (q^i_{\rm B})_0 - (q^i_{\rm A})_0 (q^i_{\rm B})_m + \sum_{k,l} \varepsilon_{mkl} (q^i_{\rm A})_k (q^i_{\rm B})_l,\\
Q^i_{m0} &= (q^i_{\rm A})_0 (q^i_{\rm B})_m - (q^i_{\rm A})_m (q^i_{\rm B})_0 + \sum_{k,l} \varepsilon_{mkl} (q^i_{\rm A})_k (q^i_{\rm B})_l,\\
Q^i_{mn} &= \delta_{mn}\Big[(q^i_{\rm A})_0 (q^i_{\rm B})_0 - \sum_k (q^i_{\rm A})_k (q^i_{\rm B})_k\Big] + (q^i_{\rm A})_m (q^i_{\rm B})_n\\
&\quad + (q^i_{\rm A})_n (q^i_{\rm B})_m - \sum_k \varepsilon_{mnk}[(q^i_{\rm A})_0 (q^i_{\rm B})_k + (q^i_{\rm A})_k (q^i_{\rm B})_0].
\end{aligned}
\tag{11}
$$

The author is grateful to Dr E. Bouzy for comments and the provision of diffraction patterns. This work was supported in part by the State Committee for Scientific Research (KBN-7 TO8A 054 21).

References

Altmann, S. L. (1986). *Rotations, Quaternions and Double Groups.* Oxford: Clarendon Press.
Bonnet, R. & Durand, F. (1975). *Phys. Status Solidi A*, **27**, 543–549.
Chen, F.-R. & King, A. H. (1987). *J. Electr. Microsc. Tech.* **6**, 55–61.
Gemperle, A. & Gemperlová, J. (1995). *Ultramicroscopy*, **60**, 207–218.
Goringe, M. J., Loberg, B. & Smith, D. A. (1979). *Phys. Status Solidi A*, **55**, 569–572.
Krieger Lassen, N. C. (1995). *J. Microsc.* **181**, 72–81.
Morawiec, A., Fundenberger, J.-J., Bouzy, E. & Lecomte, J.-S. (2002). *J. Appl. Cryst.* **35**, 287.
Morawiec, A. & Pospiech, J. (1989). *Texture Microstruct.* **10**, 211–216.
Prior, D. J. (1999). *J. Microsc.* **195**, 217–225.
Sun, S., Adams, B. L. & King, W. E. (2000). *Philos. Mag. A*, **80**, 9–25.
Wilkinson, A. J. (2001). *Scr. Mater.* **44**, 2379–2385.
Zaefferer, S. (2000). *J. Appl. Cryst.* **33**, 10–25.